Numerical investigation of magnetic sensor for DNA hybridization detection using planar transformer

Sayyed M. Azimi*, Mohammad R. Bahmanyar, Massoud Zolgharni and Wamadeva Balachandran
School of Engineering and Design, Brunel University, Uxbridge, Middlesex, UB8 3PH, UK
*Corresponding Author: E-mail: mohamad.azimi@gmail.com
Tel:+44 7985 949450

ABSTRACT
This paper introduces a sensor for detection of DNA hybridization and investigates its performance by means of computer simulation. A planar transformer with spiral windings is proposed for hybridization detection. In order to detect the occurrence of hybridization, single strand target DNA's are tagged with magnetic beads. Target DNA's are then exposed to known single strand probe DNA's which are immobilized on the surface of a functionalized layer in the proximity of the sensor. The primary winding of the transformer is driven by an AC current source. The voltage at the secondary winding is used for detection. Once the hybridization is occurred, a layer of magnetic material is formed and the coupling between the windings is varied. These variations are reflected into the detecting output voltage. The magnitude of the output voltage is numerically calculated in terms of geometrical and physical parameters and the parameter values resulting in maximum response are derived.

Keywords: DNA hybridization; Magnetic beads; Planar transformer

1. INTRODUCTION

Almost all DNA detection techniques are based on the detection of DNA hybridization. DNA consists of two long chains of subunits which are called nucleotides. Each nucleotide could be one of four chemical constituents called bases. These four bases are Adenine (A), Thymine (T), Guanine (G), and Cytosine (C). Adenine is complementary to Thymine and Guanine is complementary to Cytosine. Therefore, if all bases in one strand of DNA are complementary to all bases on the other strand of DNA then these two strands of DNA are complementary. Binding of two complementary strand of DNA which leads to construction of DNA double-strand helix is called hybridization of DNA. Bindings between DNA base pairs are very stable in room and body temperatures. Increasing the temperature to around 84 C breaks these bonds and make the DNA single-stranded. This is known as denaturing the DNA.

Traditionally, DNA hybridization detection is performed by using fluorescent tagging and optical read-out techniques. These techniques are efficient in conventional biology labs where specific protocols are followed by skilled technicians using expensive equipment.

Moreover, conventional detection of DNA is a time consuming procedure which adds an extra cost to the whole process. To overcome these problems, considerable effort has been made for more than a decade to miniaturize and integrate the whole processes in a single disposable chip. Although detection of DNA by optical methods is reliable and well practised, it cannot be easily implemented on electronic chips. Alternative methods with potential for miniaturization have been investigated in recent years. Among these methods are electrochemical techniques [1], piezoelectric sensors [2], impedance based techniques [3], field effect transistor [4, 5], capacitance techniques [6] and magnetic methods [7].

Magnetic detection methods which are based on using Micron-sized magnetic beads have been the subject of research in recent years [7–9]. These magnetic beads are normally attached to DNA strands as labels. In this way, the problem of DNA detection is reduced to detecting the magnetic beads. Using magnetic beads in DNA detection has a number of advantages. Most important of all is the fact that the biological entities existing in the solution are usually not of magnetic nature and therefore do not affect the detection process. Moreover, the magnetic properties of the beads are very stable over time and are not affected by the chemical reagents. On the other hand, using magnetic beads allows easy manipulation of DNA and therefore may be used to facilitate hybridization, mixing and separation processes [10, 11]. In particular, through application of a magnetic force, magnetic beads may also be used in non-specific bindings as well as SNPs. It is worth mentioning that using magnetic beads is not restricted to DNA and can be equally used for other biological entities. This paper introduces a DNA hybridization detection sensor that uses magnetic beads attached to DNA strands as detectable particles. Increased concentration of magnetic beads due to DNA hybridization is detected in the form of inductance variations. The response of a planar spiral mutual inductor to different types of magnetic beads is investigated and the effects of coil geometry on the performance of the sensor are numerically evaluated.

2. METHODOLOGY

The concept of using a planar transformer for DNA hybridization detection is illustrated in Figure 1. The core of the sensor is a planar spiral transformer which is sandwiched between an insulating layer on the top and a layer of permalloy in the bottom. The insulating layer is covered with a functionalized layer to which probe DNAs can attach and be immobilized. This layer could be any of standard surface treatments on gold coating or SiO_2–Si_3N_4. Magnetic beads functionalized with target DNAs are applied to this surface. Specific Hybridization of target and probe DNA will result in formation of a layer of magnetic beads above this surface. This layer is of high magnetic permeability and acts as one half of the magnetic core for the transformer. The underlying permalloy layer acts as the other half of the magnetic core and completes the magnetic circuit. Formation of this magnetic circuit allows the magnetic flux to easily pass through and leads to an increase in the mutual inductance between the windings. This property is used for detection of hybridization process.

The mutual inductor may be realized in different ways. Among different possible types of planar transformers, three types are more common and are illustrated in Figure 2. Figure 2a shows a concentric geometry in which one winding is placed within the other. Because there is only a single turn around which windings are adjacent to each other, mutual inductance and k-factor of this configuration is small whereas the self inductance of the windings are relatively larger. In this type of transformer, the ratio of windings may be varied in order to amplify the output voltage. For this geometry, k-factors as high as 0.6 have been reported [12]. In the second transformer configuration, the primary and secondary windings are interwound to promote edge coupling of the magnetic field between the windings. This leads to higher magnetic coupling and mutual inductance which is achieved at the price of

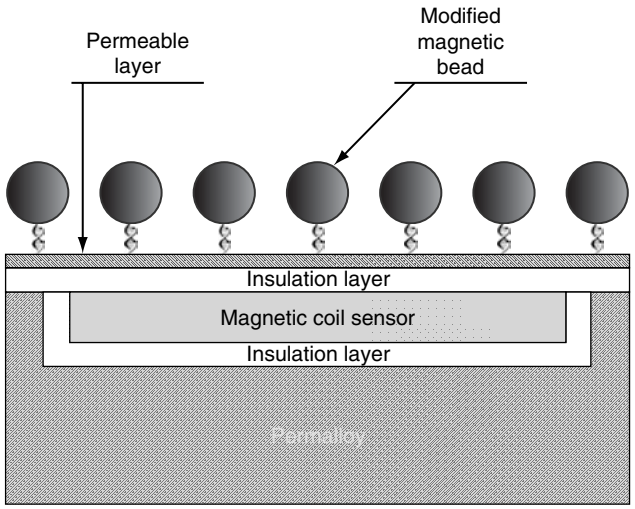

Figure 1 Proposed DNA Detection Sensor showing hybridized DNA strands tagged with magnetic beads forming a magnetically permeable layer in the proximity of coils.

reducing the self inductances of the windings due to the fact that the distance between the adjacent turns is increased in each winding. Figure 2b shows the symmetric type of this transformer which is almost like Fralan-style [13]. In this type, self-inductance in primary and secondary are the same and magnetic coupling is very high. In this type k-factors close to 0.9 could be achieved.

Figure 2c shows the stacked type transformer in which both edge and broadside magnetic coupling influence mutual inductance and k-factor [14]. The advantage of this type of windings is very high mutual inductance as well as high self-inductances. Moreover, ratio of windings could be varied to amplify voltage at secondary. Because in this type of transformer the primary and secondary windings are stacked on each other, the sensor has more thickness comparing to the other two and this subsequently reduces the overall magnitude of the signal.

2.1. ELECTRICAL MODEL OF THE SENSOR

Figure 3 shows a simplified model of a transformer. The series resistances of R_p and R_s are ohmic resistance of the conductors in the primary and secondary windings, respectively. Eqn. (1) shows the relationship between different parameters of the model.

$$\begin{pmatrix} V_{out} \\ V_{in} \end{pmatrix} = \begin{pmatrix} R_s + X_{L_s} & -X_M \\ -X_M & R_p + X_{L_P} \end{pmatrix} \begin{pmatrix} I_s \\ I_p \end{pmatrix} \tag{1}$$

If the primary is connected to an AC current source and the secondary voltage is measured by a high impedance device, the secondary current $I_s = 0$ and the Eqn. (1) reduces to:

$$V_{out} = -X_M I_p \tag{2}$$

Where $X_M = \omega M$ is the reactance due to the mutual inductance M. Eqn. (2) gives the secondary voltage which depends on X_M and I_P. Since I_P is constant, the measured secondary voltage is a

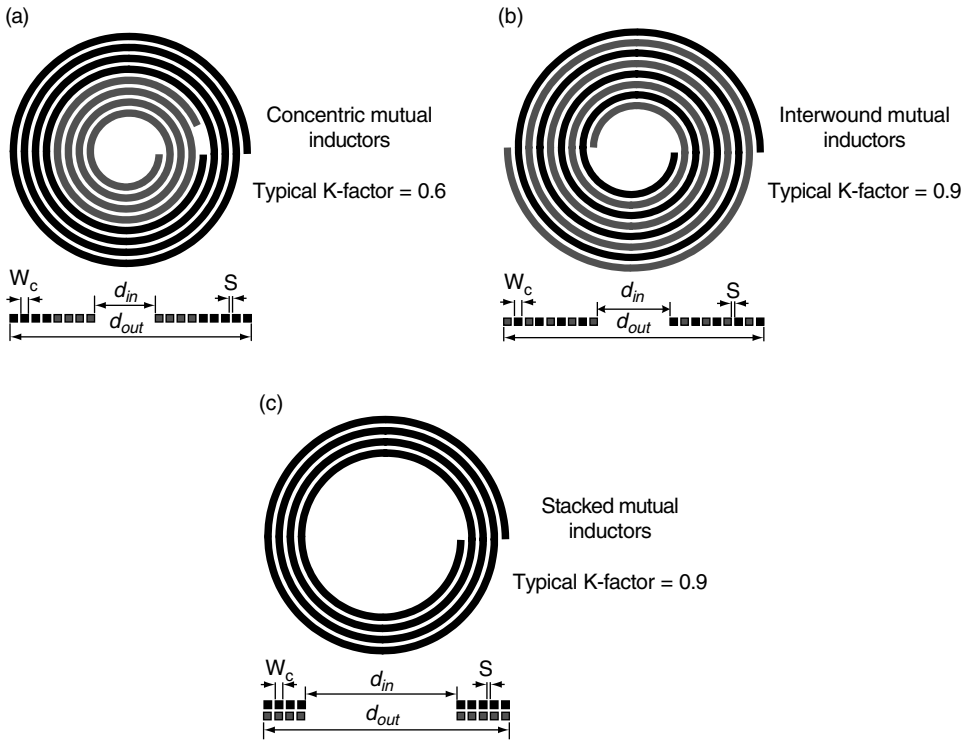

Figure 2 Common types of planar coupled inductors. Coupled inductor with (a) concentric windings (b) inter-wound windings and (c) stacked windings.

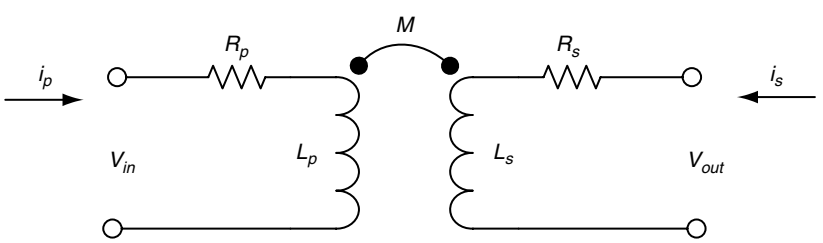

Figure 3 Electrical model of the coupled inductor showing resistances and inductances of primary and secondary windings.

direct measure of mutual inductance M. Mutual inductance may be expressed in terms of the self inductances of primary and secondary windings and coupling factor k_m as follows:

$$M = k_m \sqrt{L_p L_s} \tag{3}$$

If the transformer configuration of Figure 2b is adopted, the primary and secondary self inductances are equal ($L_p = L_s$) and Eqn. (3) reduces to:

$$M = k_m L_p \tag{4}$$

Substituting M from Eqn. (4) into Eqn. (2) yields:

$$V_{out} = -k_m X_{L_p} I_p \tag{5}$$

As is expressed in Eqn. (5), the output voltage is directly proportional to the primary (or secondary) reactance as well as the coupling factor k_m.

Based on this result and through computer simulation, the output voltage is calculated for coils of different diameters and conductor thicknesses and optimum performance of the sensor has been obtained for magnetic beads of different permeabilities.

3. SIMULATION RESULTS AND DISCUSSION

Based on the described concept, a three dimensional model of the sensor was simulated using the finite element package COMSOL FEMLAB Multiphysics v.3.2. Details of the model used in the simulation are shown in Figure 4. The model was simulated for magnetic beads as a layer with effective thickness of 2μm and different relative permeabilities.

As described in the previous section, the output voltage represents the amount of magnetic beads accumulated above the coils. On the other hand, it was shown that the output voltage was directly proportional to the self inductance of the primary winding. Therefore, the normalized change in the self inductance is chosen to evaluate the response of the sensor. In general, the coil inductance is a function of the parameters d_{out}, μ_{rB} and t_c which are defined as the outer diameter of the coil, relative permeability of magnetic beads and conductor thickness respectively. The normalized change in the inductance is then defined as follows:

$$\delta_L = \frac{L(d_{out}, t_c, \mu_{rB}) - L(d_{out}, t_c, \mu_{rB} = 1)}{L(d_{out}, t_c, \mu_{rB} = 1)} \tag{6}$$

The variations of δ_L with respect to d_{out} was simulated for different values of μ_{rB}. Other parameters as specified in Figure 4 are defined in Table 1 and the simulation results are shown in Figure 5. As shown in this figure, for each value of the relative permeability, the sensor output is maximum at a specific value of d_{out} which may be denoted as $D_{\max}$. It should be noted that the value of $D_{\max}$ is increasing with respect to μ_{rB} as shown by the dashed curve in Figure 5. To minimize the effect of permalloy on the signal, a very thick layer of permalloy (μ_{rp} = 100 μm) has been used. Also a large space-domain (7mm × 14mm) has been adopted in order to minimize computational errors.

In order to design a sensor with maximum response, it is useful to have the optimal coil diameter $D_{\max}$ in terms of different bead permeabilities and conductor thickness. The graphs in the Figure 6a shows the results of simulation for $D_{\max}$ in terms of μ_{rB} and t_c. Once the optimal diameter of the coil and the conductor thickness is known, it is useful to evaluate the magnitude of the output signal. This information may be derived from the graphs of Figure 6b which depict the maximum change $\Delta_{L\max} = \delta_L$ ($at\ D_{\max}$) corresponding to optimal values of $D_{\max}$ in terms of bead permeability and conductor thickness.

The results presented in Figure 6a shows that the percentage change in the magnitude of the proposed sensor output may be quite substantial. In comparison to the performance of GMR sensors, recently reported to have a maximum of 15% change in their output [9], the proposed sensor is capable of producing a larger response for a wide range of bead permeabilities.

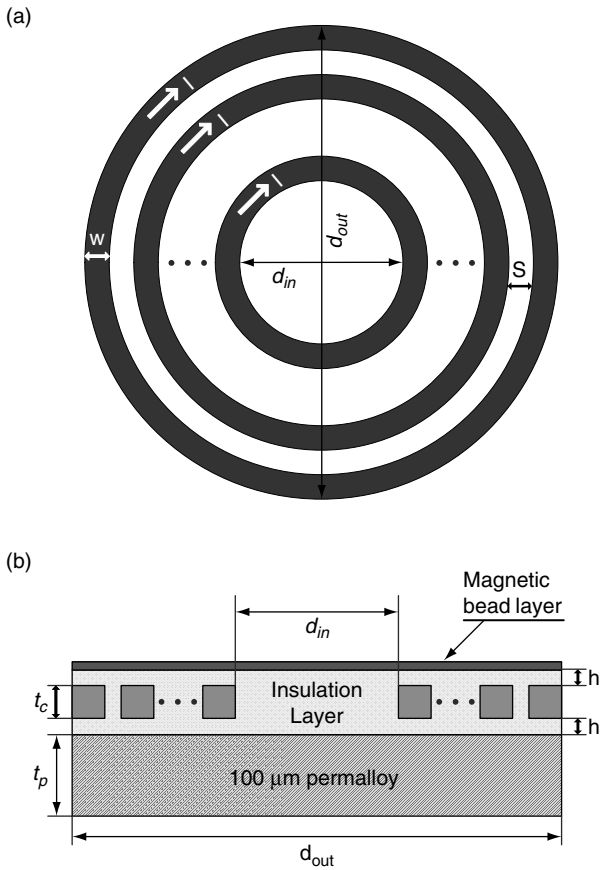

Figure 4 Sensor model used in simulations showing geometrical details of the coil and other layers (a) Top view of the coil windings (b) Lateral cross section of the sensor model.

Table 1 Various parameters and their corresponding values that are used in coupled inductors simulation.

Parameter	Explanation	Quantity
t_c	Thickness of Conductor	20 μm
w_c	Width of Conductor	20 μm
s	Space Between Conductors	30 μm
FF	Fill Factor (occupied area of conductors of the coil to the total coil area)	80%
h	Gap between coil and bead layer which is filled with insulator	10 μm

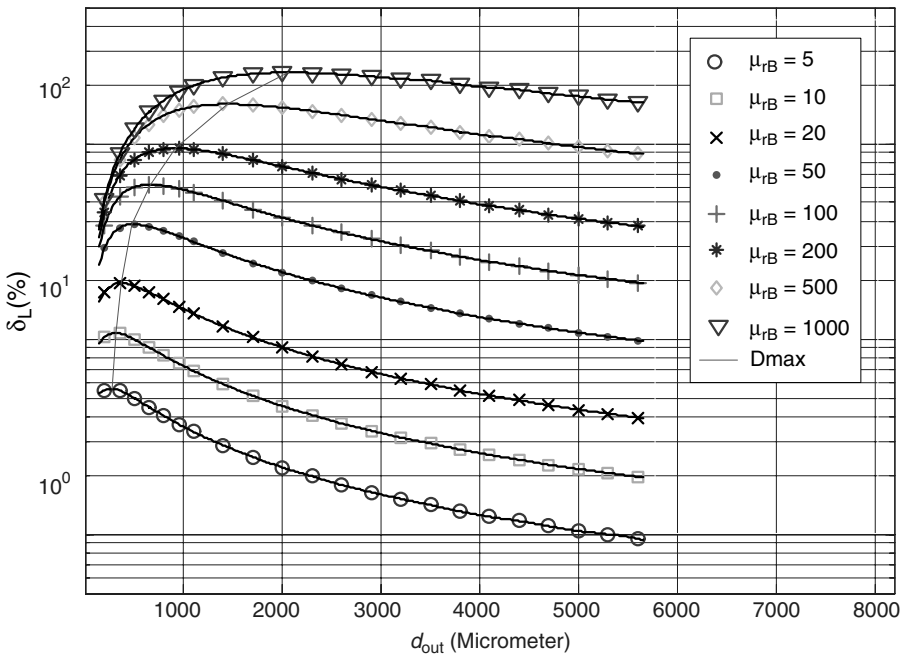

Figure 5 Behaviour of percentage change in the coil inductance against coil outer diameter for different bead permeabilities. Conductor and gap thicknesses are, $t_c = 20\mu m$, $h = 10\mu m$ respectively.

3.1. QUANTITATIVE EVALUATIONS

Based on the simulation results, an investigation was performed to find closed form expressions approximating the quantities $\Delta_{L\max}$ and $D_{\max}$ in terms of t_c and μ_{rB}. It was noted that upon doubling both t_c and μ_{rB} the values for $D_{\max}$ were doubled. Moreover, doubling one of the t_c or μ_{rB} while dividing the other by two resulted in no significant changes in $D_{\max}$. Based on these observations, it was conjectured that $D_{\max}$ may be expressed as follows:

$$D_{\max} = k_1 \sqrt{\mu_{rB}\, t_c} \tag{7}$$

The curves fitted to the simulation results based on Eqn. (7) showed satisfactory goodness of fit. In Figure 6a, the simulation results are shown as points whereas curves demonstrate the fittings.

Similarly, the following expression was proved to explain $\Delta_{L\max}$ in terms of t_c and μ_{rB}:

$$\Delta_{L\max} = k_2 \sqrt{\frac{\mu_{rB}}{t_c}} \tag{8}$$

The results of curve fitting can be seen in Figure 6b.

3.2. EFFECT OF BEAD LAYER THICKNESS

To understand the effect of bead thickness on the magnitude of signal and coil diameter, lumped parameter method is used to determine the inductance changes according to the changes in bead layer thickness. Because the magnetic beads produce a low reluctance path

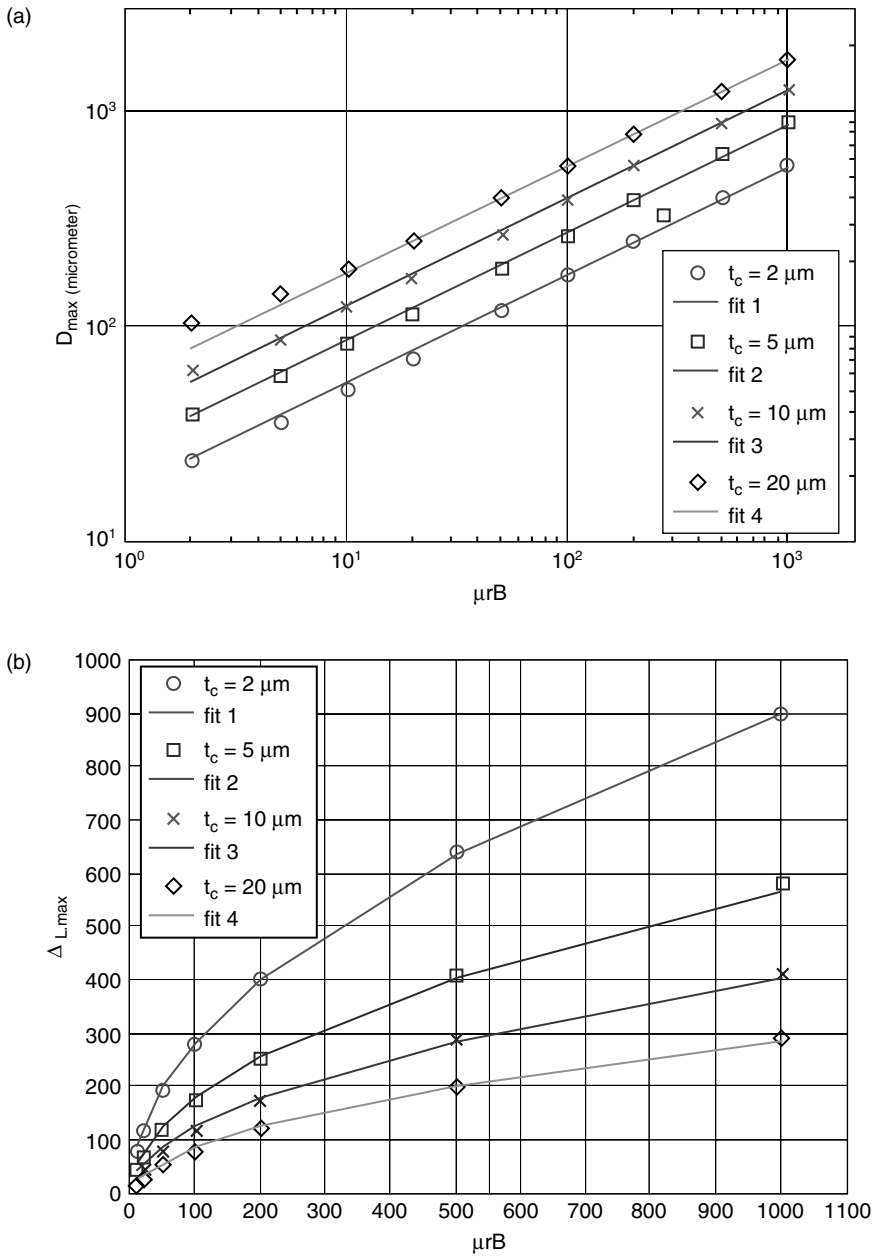

Figure 6 Graphs for determining optimal sensor parameter. (a) Outer coil diameter at which output signal is maximized against bead permeability for different conductor thickness values. (b) Corresponding maximized inductance percentage change.

for the magnetic flux of the coil, the reluctance expression may be used to investigate the effect of bead layer thickness. Assuming that the sensor surface is fully covered with magnetic beads, the magnetic reluctance of the bead layer could be expressed as [15]:

$$R_B = \frac{1}{2\pi\mu_{rB} t_B} \ln \frac{d_{out}}{d_{in}} \tag{9}$$

where R_B, t_B and d_{in} are defined as bead layer reluctance, bead layer thickness and coil inner diameter, respectively.

Lower reluctance of the bead layer allows higher magnetic flux to pass through. This results in better coupling between primary and secondary windings and therefore having a larger output. Moreover, Eqn. (9) shows that the dependence of the bead layer reluctance on both t_B and μ_{rB} is of the same form and hence it seems reasonable to introduce t_B in the expressions of $D_{\max}$ and $\Delta_{L\max}$ as follows:

$$D_{\max} = k_d \sqrt{\mu_{rB} t_c t_B} \tag{10}$$

$$\Delta_{L\max} = k_\Delta \sqrt{\frac{\mu_{rB} t_B}{t_c}} \tag{11}$$

where k_d and k_Δ are constants.

This assumption was tested against the results produced by simulation and close agreement has been confirmed.

4. CONCLUSION

It worth mentioning that the biological entities and impurities existing in the solution and on the coated surface are usually not of magnetic nature and therefore do not affect the sensitivity of the sensor. Moreover, the magnetic properties of the beads are very stable over time and are not affected by the impurities and chemical reagents. Therefore, sensitivity of the sensor is mostly a function of geometrical parameters (such as outer diameter of the coil and thickness of the coil) and physical parameters (relative permeability of the beads). After construction of the sensor geometrical parameters can not be changed therefore, the only parameter that changes the output signal is the magnetic permeability and thickness of the magnetic beads layer.

A sensor based on a planar transformer with spiral windings is introduced for detection of DNA hybridization using magnetic beads. The no-load output voltage on the secondary was taken as the sensor response while driving the primary by an AC current source. The performance of the sensor is numerically studied against the outer coil diameter, conductor thickness and different magnetic bead permeabilities. Percentage of output variations is calculated upon the formation of the magnetic bead layer and parameter values producing maximum output variations are derived and presented as design curves. Based on the numerical results, empirical formulae, which may be used for sensor design, are proposed and their validities are tested. Finally, the effect of bead layer thickness on the output is discussed and is introduced into the formulae as an extra parameter.

REFERENCES

[1] R. M. Umek et al., Electronic detection of nucleic acids, a versatile platform for molecular diagnostics, *J. Molecular Diagnostics,* 2001, vol. 3, 74–84.

[2] T. Tatsuma, Y. Watanabe, N. Oyama, K. Kitakizaki, and M. Haba, Multichannel quartz crystal microbalance, *Anal. Chem.,* 1999, vol. 71 (17), 3632–3636.

[3] F. Patolsky, A. Lichtenstein, I. Willner, Highly sensitive amplified electronic detection of DNA by biocatalyzed precipitation of an insoluble product onto electrodes, *Chemistry – A European Journal,* 2003, vol. 9, 1137–1145.

[4] E. Souteyrand, J. P. Cloarec, J. R. Martin, C. Wilson, I. Lawrence, S. Mikkelsen, and M. F. Lawrence, Direct detection of the hybridization of synthetic homo-oligomer DNA sequences by field effect, *J. Phys. Chem. B,* 1997, vol. 101, 2980–2985.

[5] J. Fritz, E. B. Cooper, S. Gaudet, P. K. Sorger, and S. R. Manalis, Electronic detection of DNA by its intrinsic molecular charge, *Proc. Nat. Acad. Sci.,* 2002, vol. 99 (22), 14, 142–6.

[6] L. Moreno-Hagelsieb, P. E. Lobert, R. Pampin, D. Bourgeois, J. Remacle, D. Flandre, Sensitive DNA electrical detection based on interdigitated Al/Al2O3 microelectrodes, *Sens. Actuators B, Chem.,* 2004, vol. 98, 269–274.

[7] P. A. Besse, G. Boero, M. Demirre, V. Pott, and R. Popovic, Detection of a single magnetic microbead using a miniaturized silicon Hall sensor, *Appl. Phys. Lett.,* 2002, vol. 80, 4199–4201.

[8] D. R. Baselt, G. U. Lee, M. Natesan, S. W. Metzger, P. E. Sheehan, and R. J. Colton, A biosensor based on agnetoresistance technology, *Biosens. Bioeleectron.,* 1998, vol. 13 (7-8), 731–739.

[9] J. C. Rife, M. M. Miller, P. E. Sheehan, C. R. Tamanaha, M. Tondra, and L. J. Whitman, Design and performance of GMR sensors for the detection of magnetic microbeads in biosensors, *Sens. Actuators A, Phys.,* 2003, vol. 107 (3), 209–218.

[10] H. Suzuki, C. M. Ho, and N. Kasagi, A chaotic mixer for magnetic bead-based micro cell sorter, *J. Microelectromech. Syst.,* 2004, vol. 13, 779–790.

[11] J. Do, J. W. Choi, and C. H. Ahn, Low-cost magnetic interdigitated array on a plastic wafer, *IEEE Trans. Magnetics,* 2004, vol. 40, 3009–3011.

[12] W. Simbuerger, H.-D. Wohlmuth, and P. Weger, A monolithic 3.7-W Silicon power amplifier with 59% PAE at 0.9 GHz, *in Proc. ISSCC,* 1999, 230–231.

[13] E. Frlan, S. Meszaros, M. Cuhaci, and J.Wight, Computer-aided design of square spiral transformers and inductors, *in Proc IEEE MTT-S,* 1989, 661–664.

[14] M. W. Geen, G. J. Green, R. G. Arnold, J. A. Jenkins, and R. H. Jansen, Miniature multilayer spiral inductors for GaAs MMICs, *in Proc. GaAs IC Symp.,* 1989, 303–306.

[15] J. W. Choi, T. M. Liakopoulos and C. H. Ahn, An on-chip magnetic bead separator using spiral electromagnets with semi-encapsulated permalloy., *Biosens. Bioelectron.* 2001, 16, 409.